

# Pathophysiology of Technetium-99m Stannous Pyrophosphate and Thallium-201 Scintigraphy of Acute Anterior Myocardial Infarcts in Dogs

L. MAXIMILIAN BUJA, ROBERT W. PARKEY, ERNEST M. STOKELY,  
FREDERICK J. BONTE, and JAMES T. WILLERSON

*From the Departments of Pathology, Radiology, and Internal Medicine,  
Southwestern Medical School, The University of Texas Health Science Center  
at Dallas, Texas 75235*

**ABSTRACT** In 17 dogs with acute myocardial infarcts produced by ligation of the proximal left anterior descending coronary artery, a comparative study was made of myocardial scintigrams obtained with technetium-99m stannous pyrophosphate ( $^{99m}\text{Tc-PYP}$ ) and thallium-201 ( $^{201}\text{Tl}$ ), tissue levels of  $^{99m}\text{Tc-PYP}$  and  $^{201}\text{Tl}$  uptake, histopathologic alterations, and regional myocardial perfusion measured with radioactive microspheres. 9 of the 10 hearts examined histologically had transmural infarcts with outer peripheral, inner peripheral, and central zones characterized by distinctive histopathologic features. A progressive reduction in myocardial blood flow was demonstrated between normal myocardium and the centers of the infarcts, and correlated well with progressive reduction in  $^{201}\text{Tl}$  uptake in the same regions. Marked  $^{99m}\text{Tc-PYP}$  concentration occurred in areas with partial to homogeneous myocardial necrosis and residual perfusion located in the outer peripheral regions of the infarcts. The latter areas also were characterized by the presence of muscle cell calcification. The patterns of distribution of  $^{99m}\text{Tc-PYP}$  and  $^{201}\text{Tl}$  explained the filling defects on  $^{201}\text{Tl}$  myocardial scintigrams and the doughnut patterns on  $^{99m}\text{Tc-PYP}$  myocardial scintigrams in dogs with transmural infarcts. One dog with a subendocardial infarct had a small homogeneous area of activity on the  $^{99m}\text{Tc-PYP}$  myocardial scintigram, and showed marked uptake of  $^{99m}\text{Tc-PYP}$  in subendocardial areas of extensive necrosis and calcification still receiving some coronary perfusion.

Thus, the data indicate that the status of regional myocardial perfusion is a key determinant for the occurrence of distinctive patterns of myocardial necrosis and for the scintigraphic detection of acute myocardial infarcts with  $^{99m}\text{Tc-PYP}$  and  $^{201}\text{Tl}$ .

## INTRODUCTION

Considerable interest has been generated in the use of myocardial scintigraphic techniques for the evaluation of patients with ischemic heart disease. Clinical and experimental studies have shown that areas of acute myocardial infarction can be identified by two basic types of scintigraphic techniques: (a) those which identify the infarcts as filling defects ("cold spots") on myocardial scintigrams (1-10), and (b) those which identify the infarcts as areas of increased radionuclide uptake ("hot spots") on myocardial scintigrams (11-18). Cold spot scintigraphy of acute myocardial infarcts has been performed with radionuclides of potassium and its analogues, including rubidium, cesium, and thallium (1-10). Hot spot scintigraphy has been performed with gallium-67 citrate (11) as well as technetium-99m tetracycline (12, 13), technetium-99m glucoheptonate (14-16), and various phosphate compounds labeled with technetium-99m (16-18), including technetium-99m stannous pyrophosphate ( $^{99m}\text{Tc-PYP}$ ).<sup>1</sup> Furthermore, an extensive clinical experience has now been compiled with  $^{99m}\text{Tc-PYP}$  (10, 18-20). The present study was undertaken to elucidate the pathophysiologic basis for the

Dr. Willerson is an Established Investigator of the American Heart Association.

Received for publication 27 September 1975 and in revised form 30 January 1976.

<sup>1</sup> Abbreviations used in this paper: LAD, left anterior descending coronary artery; PAS, periodic acid-Schiff;  $^{99m}\text{Tc-PYP}$ , technetium-99m stannous pyrophosphate;  $^{201}\text{Tl}$ , thallium-201.

scintigraphic detection of acute myocardial infarcts with  $^{99m}\text{Tc}$ -PYP and thallium-201 ( $^{201}\text{Tl}$ ) by means of studying the interrelationships between regional myocardial perfusion, tissue levels of  $^{99m}\text{Tc}$ -PYP and  $^{201}\text{Tl}$ , and histopathologic alterations in canine hearts subjected to coronary occlusion.

## METHODS

A total of 17 mongrel dogs were anesthetized with intravenous pentobarbital sodium (30 mg/kg) and underwent thoracotomy followed by ligation of the proximal left anterior descending coronary artery (LAD). In some cases, two or three prominent epicardial collateral arteries also were ligated. After closure of the thoracotomies, the dogs were allowed to awaken and were kept alive for 18–24 h (4 dogs) or 36–48 h (13 dogs). The dogs then were lightly anesthetized with pentobarbital sodium (20 mg/kg) before performance of the following studies.

Each of the 17 dogs was prepared according to one of the following protocols: (a) 9 dogs received intravenous injection of  $^{99m}\text{Tc}$ -PYP (Mallinckrodt Inc., St. Louis, Mo.) as well as  $^{201}\text{Tl}$  (New England Nuclear, Boston, Mass.); (b) 5 dogs received  $^{99m}\text{Tc}$ -PYP administered intravenously and approximately 1–3 million 15- $\mu\text{m}$  microspheres labeled with  $^{125}\text{I}$ , administered through left atrial catheters (21, 22); (c) 2 dogs were given intravenous injections of  $^{201}\text{Tl}$  only; and (d) 1 dog received an intravenous injection of  $^{99m}\text{Tc}$ -PYP only. 1–2 h after injection of 2.8–4.0 mCi of  $^{99m}\text{Tc}$ -PYP and 20–30 min after injection of 1.5–2.1 mCi of  $^{201}\text{Tl}$ , myocardial scintigrams were obtained in the anterior, left anterior oblique, and left lateral projections. The  $^{201}\text{Tl}$  and  $^{99m}\text{Tc}$ -PYP scintigrams were obtained in rapid succession from the dogs which received both radiopharmaceuticals. The scintigraphic studies were performed with a Searle Pho Gamma III HP camera with a 16,000 hole, "high resolution" collimator (Searle Radiographics Inc., Des Plaines, Ill.). The  $^{201}\text{Tl}$  myocardial scintigrams were obtained with the camera set at 80 keV with a 10% window. The camera was set at 140 keV with a 20% window for the  $^{99m}\text{Tc}$ -PYP scintigrams.

After completion of the scintigraphic studies, the dogs were sacrificed by intravenous injections of large doses of pentobarbital. Intervals between injection and sacrifice were 1½–3½ h for  $^{99m}\text{Tc}$ -PYP, 1–2½ h for  $^{201}\text{Tl}$  and 10–40 min for microspheres. Postmortem scintigraphic studies were performed on the whole hearts of four dogs which had received injections of both  $^{201}\text{Tl}$  and  $^{99m}\text{Tc}$ -PYP. Each of the four hearts were positioned sequentially, in the anteroposterior, left anterior oblique, and left lateral positions, and  $^{99m}\text{Tc}$ -PYP and  $^{201}\text{Tl}$  myocardial scintigrams were obtained while the hearts were kept in each position. Postmortem scintigraphy also was performed with specimens obtained from three additional dogs, of which two had received only  $^{201}\text{Tl}$  and one only  $^{99m}\text{Tc}$ -PYP. These three hearts were divided into multiple transverse slices, and scintigrams were obtained from the individual slices.

In 10 hearts, comparative studies were made of tissue levels of radioactivity and histologic alterations. 5 of the 10 hearts were obtained from dogs given injections of  $^{99m}\text{Tc}$ -PYP and  $^{201}\text{Tl}$ , and 5 hearts were from dogs given  $^{99m}\text{Tc}$ -PYP and microspheres. The hearts were divided into multiple transverse slices. 9 of the 10 hearts were found to have large, transmural, anterior myocardial infarcts (Fig. 1), and 1 heart showed a relatively small, subendocardial anterior

infarct. 7–13, full-thickness, transmural blocks were cut from the various transverse slices of each heart (Fig. 1). These blocks were taken from the following regions: (a) grossly normal posterobasal left ventricular myocardium; (b) grossly normal right ventricular myocardium (two hearts); (c) anterior infarcted myocardium; (d) infarcted myocardium intermediate in location between the anterior regions and lateral or septal edges of the infarcts; and (e) myocardium containing the grossly identifiable lateral or

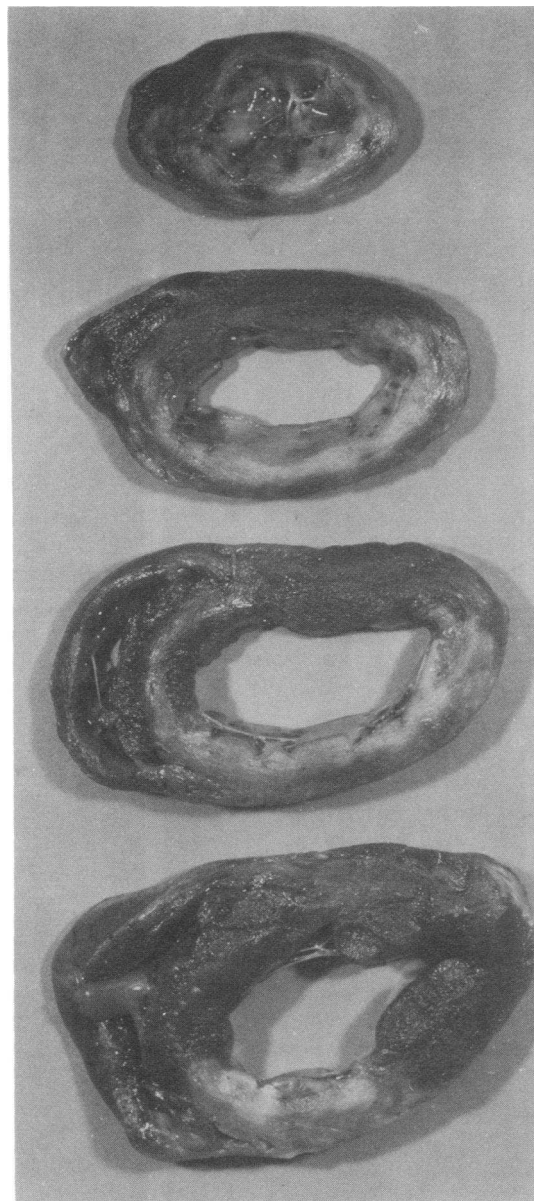
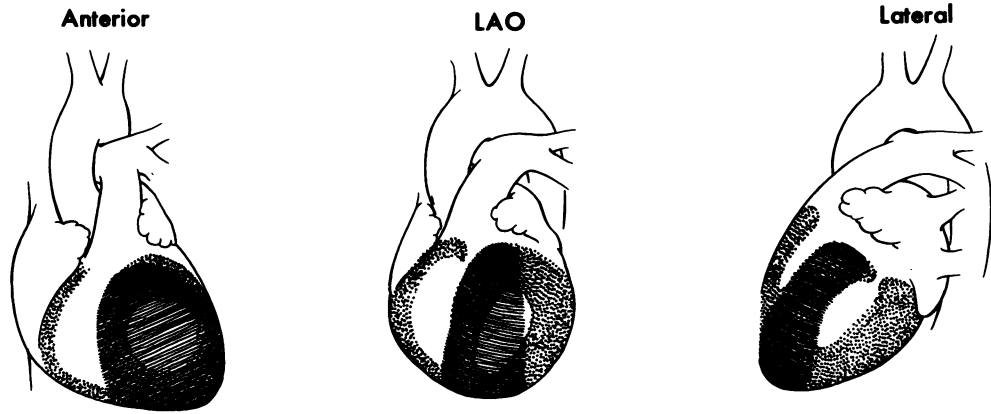
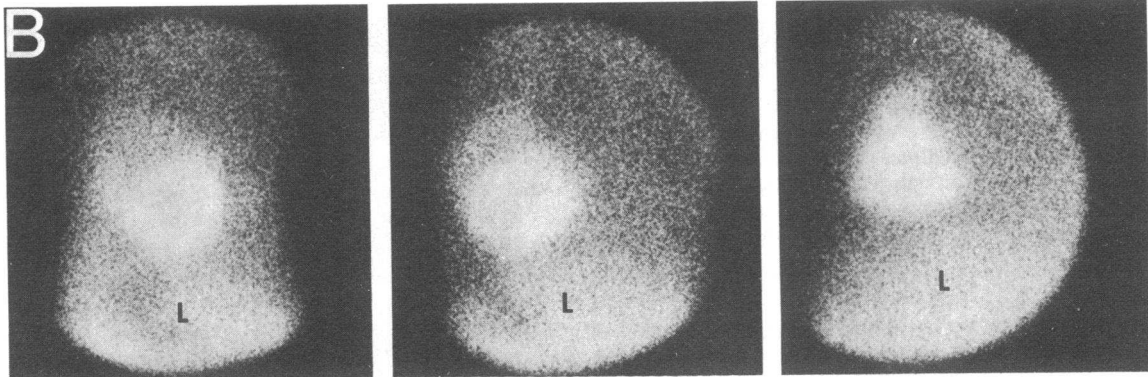


FIGURE 1 Transverse sections of the ventricles of a canine heart with a large transmural acute anterior myocardial infarct produced by ligation of the proximal left anterior descending coronary artery for 42 h. Note that the infarct extends further laterally and septally as the apex is approached and is almost circumferential at the apex.

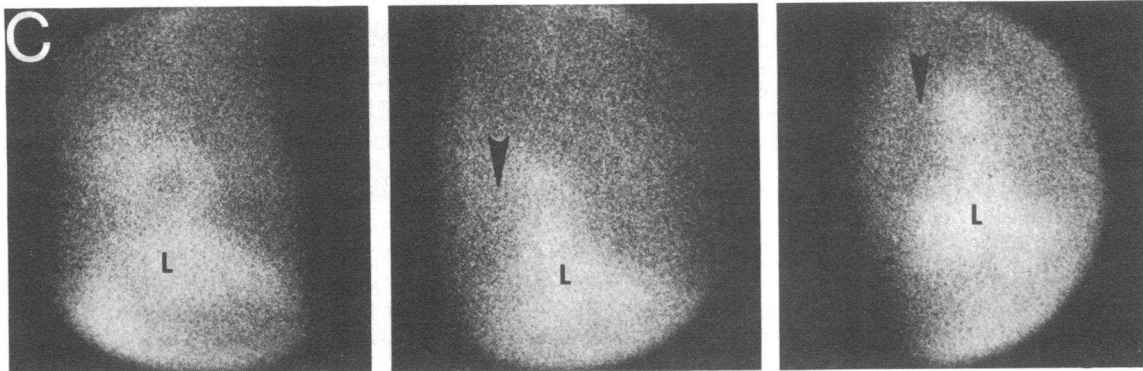
**A**



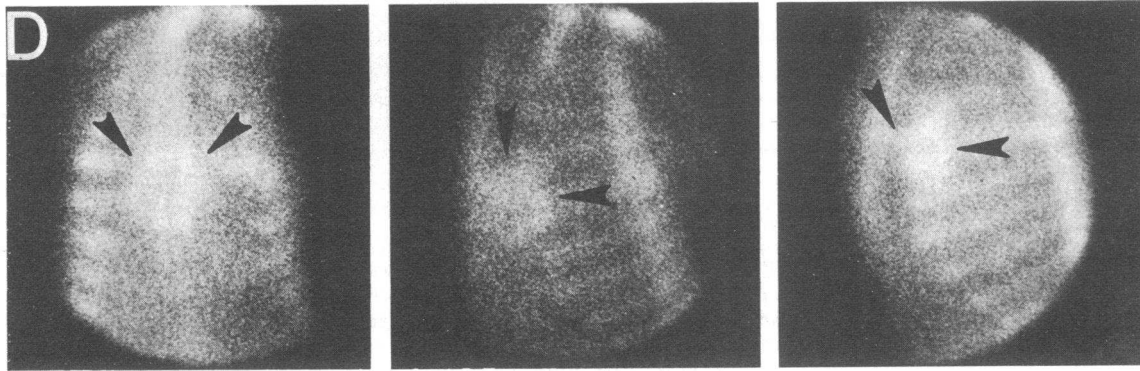
**B**



**C**



**D**



septal edges of the infarcts. Thin transmural sections were cut from the top (basal) and bottom (apical) surfaces of each block, fixed in 10% phosphate-buffered formalin (pH 7.4) for 1–2 days, and processed for histologic study. The remaining portion of each block was divided into four, approximately equal, samples: an immediately subepicardial quarter, an outer middle quarter, an inner middle quarter, and an immediately subendocardial quarter. The samples were placed in airtight tubes and their weights obtained. The weights of most samples were in the range of 50–200 mg.

The tissue samples were assayed for radioactivity in a Searle well-type scintillation counter (Searle Analytic Inc., Des Plaines, Ill.) or in a Scientific Products Gamma scintillation counter (Scientific Products Inc., State College, Pa.). Counts were obtained from regions of interest centered around the peak energy levels of  $^{99m}\text{Tc}$  gamma ray (140 keV), the  $^{201}\text{Tl}$  X ray (80 keV), and the  $^{125}\text{I}$  X ray (35 keV). Background counts at each of these settings also were obtained and subtracted from total counts. 1-min counting intervals were employed for  $^{99m}\text{Tc}$  and  $^{201}\text{Tl}$ , and 3-min intervals were used for  $^{125}\text{I}$ .

In samples containing  $^{99m}\text{Tc}$ -PYP and  $^{125}\text{I}$ -microspheres,  $^{99m}\text{Tc}$  radioactivity was analyzed within 6–12 h after injection of radionuclides, and  $^{125}\text{I}$  activity was determined 3–5 days later. In the samples containing  $^{99m}\text{Tc}$ -PYP and  $^{201}\text{Tl}$ , tissue levels of radioactivity were recorded from the 140-keV and 80-keV regions within 6–12 h after injection of the radionuclides, and then corrected for the relative amounts of  $^{99m}\text{Tc}$ -PYP and  $^{201}\text{Tl}$  radioactivity. The raw  $^{201}\text{Tl}$  counts were corrected for down-scattered  $^{99m}\text{Tc}$  counts according to the following formula utilizing a  $^{99m}\text{Tc}$  standard, analyzed at both the 80-keV and 140-keV regions of interest:  $^{201}\text{Tl}$  counts = Total sample counts at 80 keV – ( $^{99m}\text{Tc}$ -PYP sample counts at 140 keV  $\times$  [ $^{99m}\text{Tc}$  standard at 80 keV /  $^{99m}\text{Tc}$  standard at 140 keV]). The  $^{99m}\text{Tc}$  counts at 80 keV amounted to only 1% of the  $^{99m}\text{Tc}$  activity at 140 keV, and accounted for less than 10% of total counts in the  $^{201}\text{Tl}$  region of interest.  $^{201}\text{Tl}$  counts also were obtained 3–5 days after the dogs were sacrificed. At this time, tissue samples were free of significant  $^{99m}\text{Tc}$  radioactivity ( $^{99m}\text{Tc}$  has a half-life of 6.0 h). Comparison of the corrected  $^{201}\text{Tl}$  counts obtained on the day of sacrifice and the  $^{201}\text{Tl}$  counts obtained 3–5 days later revealed no significant differences in the relative levels of  $^{201}\text{Tl}$  per unit weight in the various samples.

The raw  $^{99m}\text{Tc}$ -PYP counts were corrected for radioactivity from  $^{201}\text{Tl}$  gamma rays (135 and 167 keV) (7). These photons have been reported to have an abundance of 12% for each  $^{201}\text{Tl}$  disintegration (7). Tests with standards

in our system also confirmed this 12% figure. Therefore, the raw  $^{99m}\text{Tc}$ -PYP counts from the tissue samples were corrected according to the following formula:  $^{99m}\text{Tc}$ -PYP counts = Total sample counts at 140 keV – (corrected  $^{201}\text{Tl}$  counts  $\times$  0.12).

For each sample, data were expressed as  $^{99m}\text{Tc}$  counts/g per min,  $^{201}\text{Tl}$  counts/g per min, and (or)  $^{125}\text{I}$  counts/g per 3 min. An average, weight-corrected, normal value for  $^{99m}\text{Tc}$ ,  $^{201}\text{Tl}$ , or  $^{125}\text{I}$  activity for each heart was calculated by averaging the values from the four samples obtained from normal posterobasal left ventricular myocardium and, in two hearts, the samples obtained from normal right ventricular myocardium. Abnormal-to-normal ratios of radioactivity were calculated for each radioisotope in each sample using the average normal values determined for the given radioisotope in each heart. Statistical analysis of the data was performed using the paired *t* test or group *t* test; differences were considered significant when  $P < 0.05$ .

For the morphologic studies, histologic sections were prepared from the basal and apical slices obtained from each block. The sections were stained with: (a) hematoxylin and eosin; (b) the periodic acid-Schiff (PAS) technique, with and without prior digestion with diastase for removal of glycogen deposits (23); and (c) the von Kossa silver nitrate technique for calcium salts (23).

## RESULTS

**Scintigraphic findings.** Interpretation of the  $^{99m}\text{Tc}$ -PYP and  $^{201}\text{Tl}$  myocardial scintigrams in the 17 dogs with proximal LAD occlusion was based on our previous experience with  $^{99m}\text{Tc}$ -PYP and  $^{201}\text{Tl}$  myocardial scintigraphy in dogs and patients with and without clinicopathologic evidence of ischemic heart disease (10, 16–20). Normal  $^{99m}\text{Tc}$ -PYP scintigrams, obtained at least 1 h after injection of the radionuclide, are characterized by visualization of marked activity in the skeletal system and no detectable activity in the regions of the heart or liver. Normal  $^{201}\text{Tl}$  scintigrams show marked activity in the regions of the heart and liver and no activity in the skeletal system (Fig. 2). Myocardial uptake of  $^{201}\text{Tl}$  occurs in the form of a circular area of intense activity corresponding to a critical mass of left ventricular myocardium positioned perpendicular to the scintigraphic camera in a given projection (Fig. 2). Right ventricular myocardium also is visualized under optimal circum-

FIGURE 2 Typical scintigraphic findings obtained with  $^{201}\text{Tl}$  and  $^{99m}\text{Tc}$ -PYP. On the illustrative diagram (row A), the areas depicted by dots correspond to critical masses of normal right and left ventricular myocardium which are visualized as regions of intense activity on the normal  $^{201}\text{Tl}$  scintigram obtained in a dog not subjected to coronary occlusion (row B); the central areas of decreased activity represent the ventricular cavities. The area of the heart depicted by slash lines represents a large acute anterior myocardial infarct. The infarct is visualized as a filling defect (arrowheads) in the left anterior oblique and lateral projections of the positive  $^{201}\text{Tl}$  myocardial scintigram obtained from a dog 42 h after LAD occlusion (row C; Dog 3, Table I). The lesion is not well visualized on the anterior projection due to superimposition of activity from normal posterior myocardium. The same infarct is visualized as an area of intense radioactivity (arrowheads) in all three projections of the  $^{99m}\text{Tc}$ -PYP scintigram (row D). A doughnut pattern due to a central area of decreased activity is seen on the anterior projection of the  $^{99m}\text{Tc}$ -PYP scintigram. In addition to myocardial activity, the  $^{201}\text{Tl}$  scintigrams show activity in the liver (L), and the  $^{99m}\text{Tc}$ -PYP scintigrams show activity in skeletal structures, including sternum, spine, and ribs.

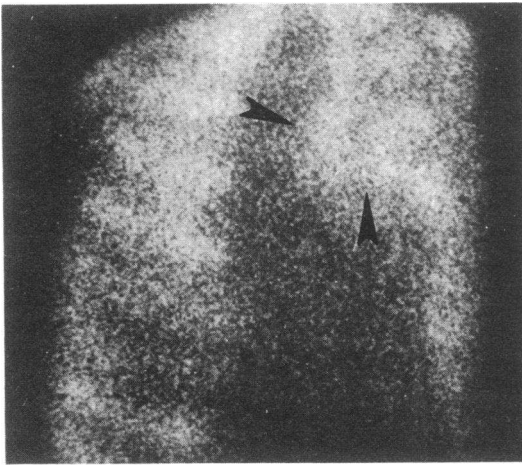


FIGURE 3  $^{99m}\text{Tc}$ -PYP scintigram from a dog with an acute anterior subendocardial infarct 42 h old. An area of homogeneous  $^{99m}\text{Tc}$ -PYP activity (arrowheads) is present in this region of the heart.

stances. Central areas of decreased activity represent the ventricular cavities.

All  $^{201}\text{Tl}$  and  $^{99m}\text{Tc}$ -PYP myocardial scintigrams were abnormal in the dogs subjected to proximal LAD occlusion (Fig. 2). Scintigraphy of the dogs given both  $^{99m}\text{Tc}$ -PYP and  $^{201}\text{Tl}$  resulted in only slight deterioration in image quality. The  $^{201}\text{Tl}$  myocardial scintigrams exhibited filling defects corresponding to the sites of anterior myocardial infarcts. Comparison with normal  $^{201}\text{Tl}$  myocardial scintigrams showed that the filling defects were clearly identifiable only in the left anterior oblique

and lateral projections, and were not well-visualized in the anterior projections, presumably as a result of superimposition of activity from normal posterior myocardium. Positive  $^{99m}\text{Tc}$ -PYP myocardial scintigrams in most dogs showed a characteristic "doughnut" pattern in the anterior projection, with radioactivity concentrated peripherally around a central area of relatively decreased radioactivity (Fig. 2). In contrast, the myocardial scintigram in the one dog with a subendocardial infarct showed a homogeneous area of  $^{99m}\text{Tc}$ -PYP activity (Fig. 3).

Postmortem scintigraphy of four whole hearts from dogs given both  $^{99m}\text{Tc}$ -PYP and  $^{201}\text{Tl}$  revealed the same patterns observed in vivo. In these scintigrams, however, partial overlap in the distribution of  $^{99m}\text{Tc}$ -PYP and  $^{201}\text{Tl}$  activities was clearly demonstrable, even in the lateral projection, where overlapping of normal and infarcted myocardium was minimized (Fig. 4). For the four hearts, the areas of overlapping  $^{201}\text{Tl}$  and  $^{99m}\text{Tc}$ -PYP activity were 44.7, 44.8, 48.7, and 38% of the total areas of  $^{99m}\text{Tc}$ -PYP activity on the lateral projections, respectively.

Scintigraphy of transverse ventricular slices from one dog given only  $^{99m}\text{Tc}$ -PYP showed that significant  $^{99m}\text{Tc}$ -PYP activity was confined to the grossly identified region of infarcted myocardium and that the activity was most intense at the peripheries of the lesion (Fig. 5). Scintigraphy of ventricular slices from two dogs given only  $^{201}\text{Tl}$  revealed low, but significant, levels of activity within the regions of transmural infarction (Fig. 5).

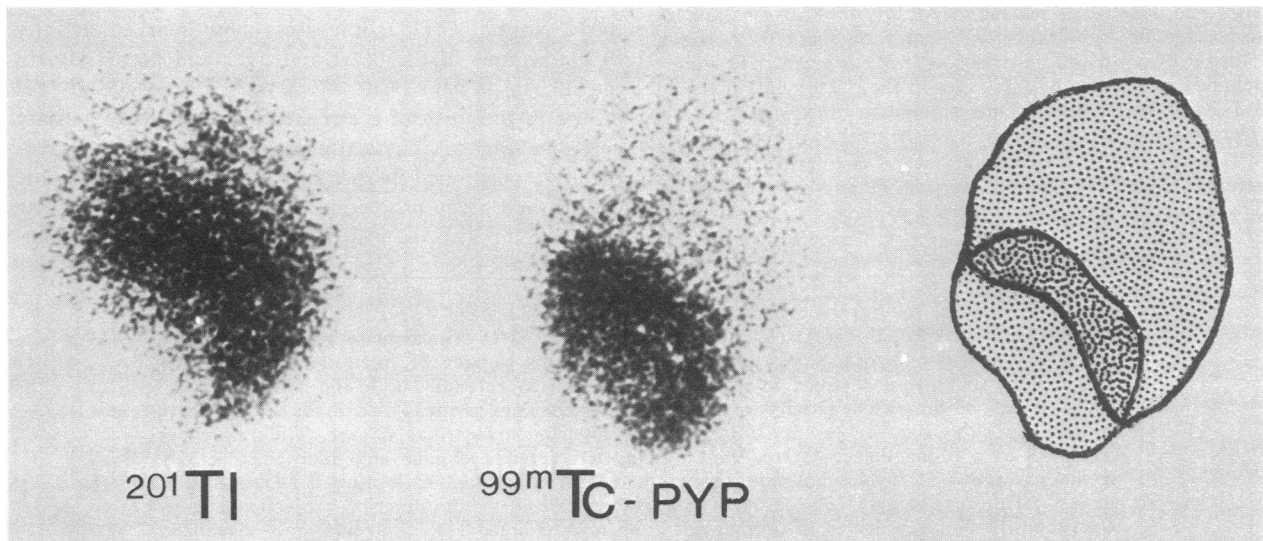


FIGURE 4  $^{99m}\text{Tc}$ -PYP and  $^{201}\text{Tl}$  scintigrams obtained in the lateral projection from a heart with a 2-day-old, large, anterior myocardial infarct after removal of the heart at necropsy. A large area with overlapping  $^{99m}\text{Tc}$ -PYP and  $^{201}\text{Tl}$  activities is visualized by the scintigrams and illustrated in the diagram on the right.

**Morphologic findings.** Analysis of the multiple sections allowed formulation of a topographical map of the histopathologic alterations in the hearts with proximal LAD occlusions and apicoanterior myocardial infarcts (Fig. 6). 9 of the 10 hearts showed large transmural infarcts which had histopathologically distinct central, inner peripheral, and outer peripheral zones (Figs. 6–8). The central zones of the infarcts were surrounded subepicardially, subendocardially, laterally, superiorly, and inferiorly (adjacent to the cardiac apex) by the peripheral zones. 1 of the 10 hearts had a subendocardial infarct, with confluent necrosis confined to the inner half to two-thirds of the left ventricular wall and only patchy necrosis in the outer portion of the wall. This infarct lacked a central zone.

The central zones of the infarcts (Figs. 6–8) were characterized by a virtual absence of neutrophils and by the presence of a homogeneous population of necrotic muscle cells which exhibited: (a) nuclear pyknosis, palor, or lysis; (b) palely stained cytoplasm with indistinct or markedly relaxed myofibrils; (c) glycogen depletion (PAS stain); (d) faint, diffuse, diastase-resistant PAS staining; and (e) virtual absence of calcification (von Kossa stain). Variable amounts of calcium deposits, however, were present in the walls of small blood vessels, capillaries, and interstitial regions in the centers of the infarcts (Figs. 7, 8).

The peripheral zones of the transmural infarcts were extensively infiltrated with neutrophils, showed prominent vascular congestion, and contained a pleomorphic population of necrotic muscle cells (Figs. 6–9). The necrotic muscle cells exhibited certain common features, including: (a) nuclear pyknosis, palor, or lysis; (b) pale cytoplasmic staining; (c) glycogen depletion (PAS stain); and (d) moderate, diffuse, diastase-resistant PAS staining. Many of the muscle cells showed marked disruption of myofibrils associated with the presence of numerous, dense, contraction bands, whereas other muscle cells had relaxed or indistinct myofibrils. In sections stained by the von Kossa method, certain necrotic muscle cells were shown to contain variable numbers of discrete calcium deposits (Figs. 6–9).

The peripheral zones of the infarcts could be subdivided into inner and outer peripheral zones on the basis of the relative content of calcified muscle cells and neutrophils (Figs. 6–9). The inner peripheral zones contained relatively few calcified muscle cells, but did exhibit larger amounts of neutrophils than the outer peripheral zones, due to accumulation of the neutrophils at the borders between the inner peripheral and central zones. The outer peripheral zones were characterized by the presence of relatively large numbers of calcified muscle cells. Although muscle cell

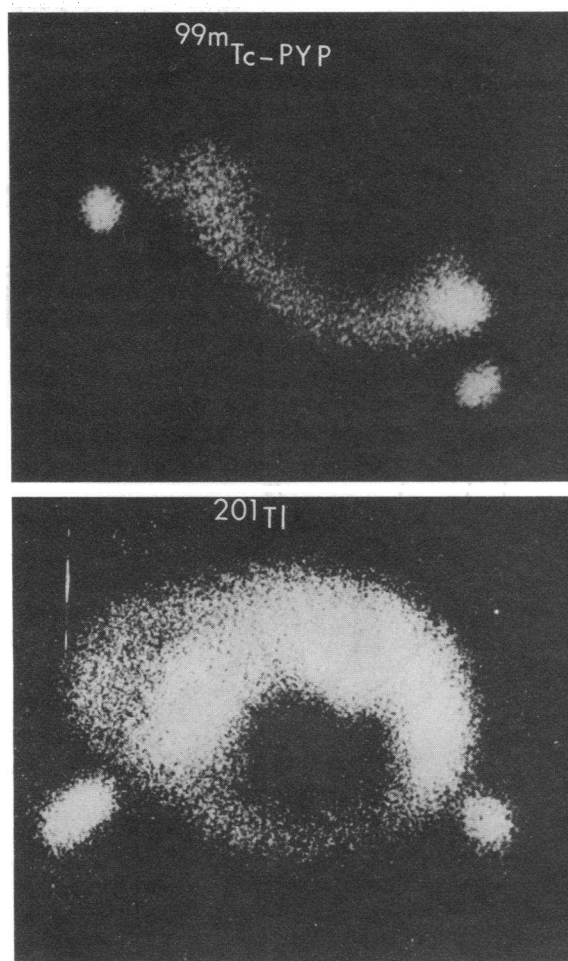


FIGURE 5 Top panel shows a scintigram of a transverse ventricular slice from a dog given  $^{99m}\text{Tc}$ -PYP only, and bottom panel shows a scintigram of a ventricular slice from a dog given  $^{201}\text{Tl}$  only. The extraneous radioactive spots are markers for the boundaries of 24-h-old areas of transmural infarction in each slice, which appeared similar to those shown in Fig. 1. Visible  $^{99m}\text{Tc}$ -PYP activity is confined to the infarcted region, is most intense at the peripheries of the lesion, and shows a central region of relatively decreased activity. On the  $^{201}\text{Tl}$  scintigram, intense activity is seen in normal myocardium, and definitely decreased but significant activity is visible in the infarcted region.

calcification was most abundant in the outer peripheral region of each infarct, the extent of muscle cell calcification in different infarcts was variable and ranged from moderate to massive (Fig. 8).

At the lateral edges of the infarcts, myocardial necrosis was patchy, and mixtures of necrotic and non-necrotic myocardium were present (Figs. 6, 9). The necrotic myocardium had features of the outer peripheral zone as described above. Non-necrotic muscle cells

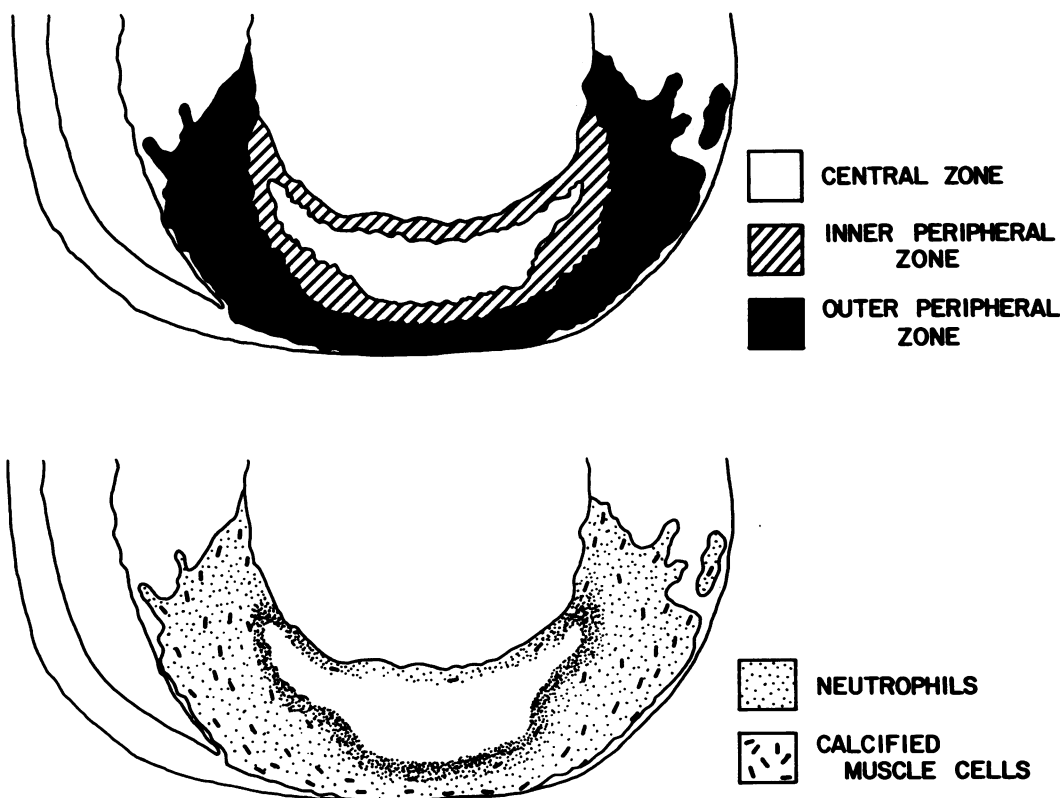


FIGURE 6 Topography of histopathologic alterations in a typical ventricular slice through a canine heart with a transmural acute anterior myocardial infarct. The infarct has outer peripheral, inner peripheral, and central zones with distinctive histopathologic features. Sections through the basal and apical edges of the infarct would not show a central zone.

showed changes indicative of significant damage, including variable degrees of nuclear pyknosis, cytoplasmic eosinophilia, decrease in glycogen content (PAS stain), and fine vacuolization suggestive of lipid accumulation. These muscle cells were devoid of calcium deposits (Fig. 9).

*Tissue levels of  $^{99m}\text{Tc-PYP}$ ,  $^{201}\text{Tl}$ , and  $^{125}\text{I}$ -microspheres.* The data regarding tissue levels of radioactivity are shown in Table I, and a statistical analysis of the data presented in Table II. The data were derived by correlating tissue levels of  $^{99m}\text{Tc-PYP}$ ,  $^{201}\text{Tl}$  and (or)  $^{125}\text{I}$  radioactivity in a given sample with the extent and histopathologic features of necrosis in the corresponding quadrant of the histologic sections. Study of sections obtained from both surfaces (apical and basal) of the tissue blocks proved important in grading the extent and nature of histopathologic changes, since the infarcts tended to extend further laterally and septally in the apical than in the basal portions of each ventricular slice (Fig. 1), and since the infarcts generally extended further laterally and septally in the sub-endocardial than in the subepicardial regions of each ventricular slice (Fig. 6). Extent of necrosis was graded

as none (0), scattered small foci (1+), moderate (2+), extensive (3+), or homogeneous (4+). When samples for well counting appeared to contain muscle with histopathologic features of more than one zone, the samples were assigned to the predominant zone.

Values for  $^{125}\text{I}$ -microspheres indicated a progressive reduction in myocardial blood flow between normal myocardium and the centers of the infarcts in four hearts with transmural infarcts. As determined by microsphere counts, average mean myocardial blood flow was 81% of normal in partially necrotic areas in the outer peripheries of the infarcts, 26% of normal in areas of extensive to confluent necrosis in the outer peripheries, 6% of normal in the inner peripheries, and 4% of normal in the centers of the infarcts.

Extent of reduction of  $^{201}\text{Tl}$  uptake in different regions of five hearts correlated well with the degree of perfusion deficit in similar regions of the four hearts used for microsphere studies. Average mean  $^{201}\text{Tl}$  uptake was 74% of normal in partially necrotic areas in the outer peripheries of the infarcts, 27% of normal in areas of extensive to confluent necrosis in the outer peripheries,

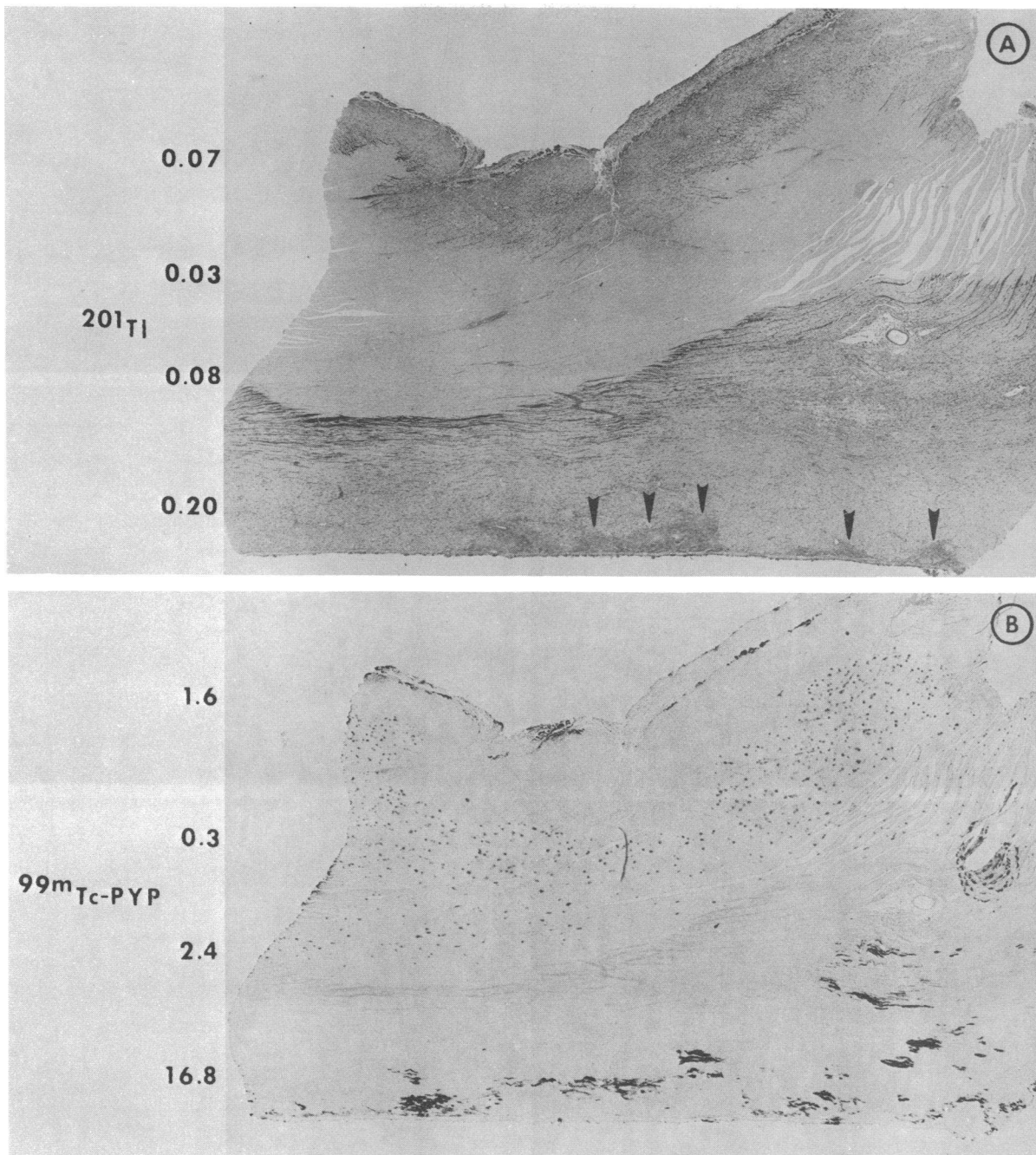


**FIGURE 7** Adjacent histologic sections stained with hematoxylin and eosin (A) and by the von Kossa method for calcium salts (B) and corresponding tissue levels (abnormal-to-normal ratios) of  $^{201}\text{Tl}$  and  $^{99\text{m}}\text{Tc-PYP}$  from a sample taken from the anterior aspect of a 42-h-old canine infarct (Dog 2, Table I). The subepicardially located myocardium belongs to the outer peripheral zone and exhibits numerous, darkly stained, necrotic, calcified muscle cells (B) as well as small foci of damaged but not demonstrably necrotic muscle cells (arrowheads; A). The inner peripheral zone contains few calcified muscle cells but numerous neutrophils concentrated around the border with the central zone (A and B). The central zone is devoid of neutrophils and calcified muscle cells, but contains small, darkly stained foci of calcification corresponding to vascular and tissue spaces (see Fig. 9). A, hematoxylin and eosin stain  $\times 18$ ; B, von Kossa stain  $\times 18$ .

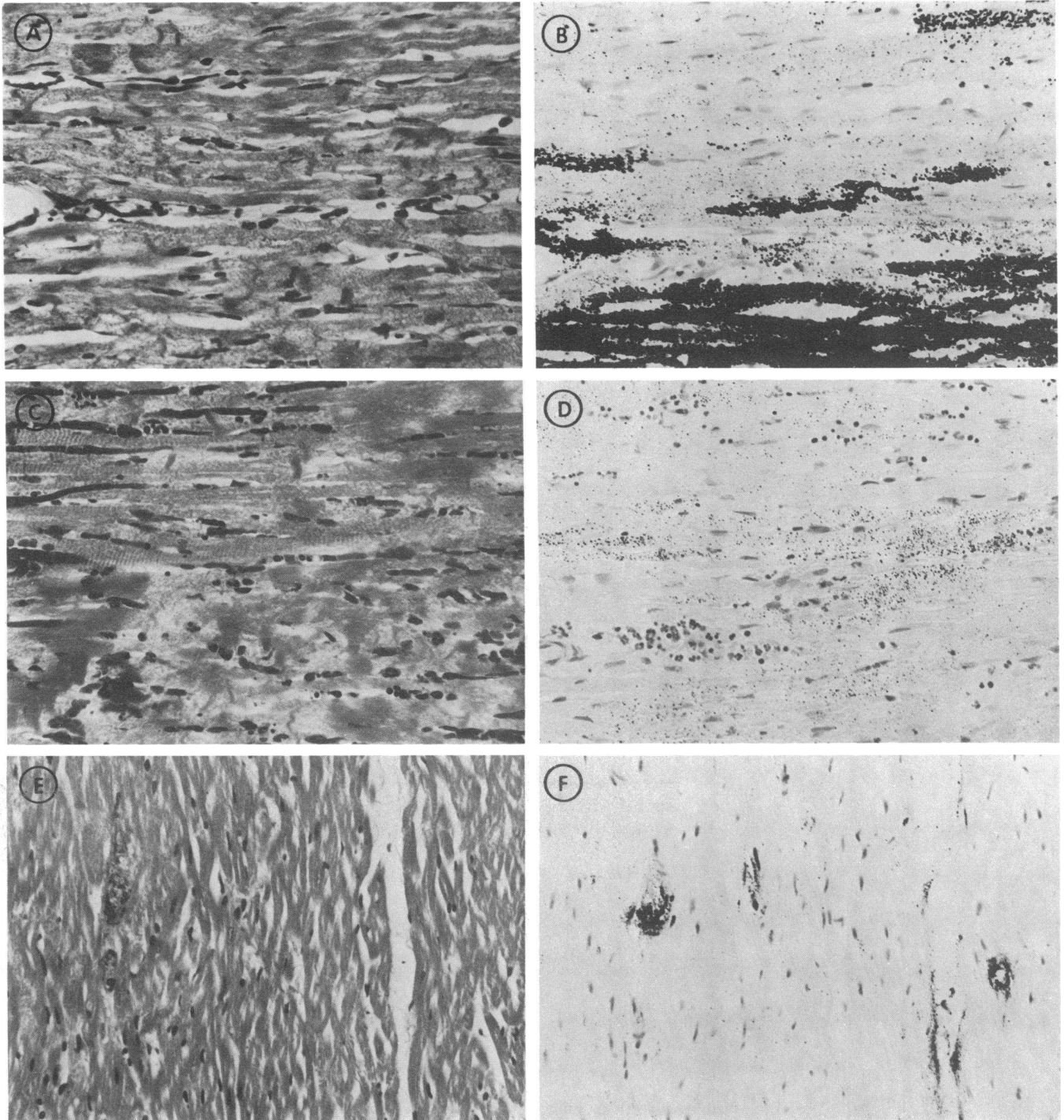


FIGURE 8 Histopathologic features of the outer peripheral zone of an infarct with marked muscle cell calcification (Dog 2, Table I; A and B), the outer peripheral zone of an infarct with mild muscle cell calcification (Dog 3, Table I; C and D) and the central zone of an infarct (Dog 2, Table I; E and F); all infarcts were 42 h old. Many muscle cells in the outer peripheral zones have disrupted myofibrils and numerous contraction bands and contain variable numbers of discrete granular calcium deposits. Muscle cells in the central zone have indistinct myofibrils and are devoid of calcium deposits. Calcification, however, is present in the walls of small blood vessels and along a tissue space. A, C, and E, hematoxylin and eosin stain; B, D, and F, von Kossa stain; all  $\times 300$ .

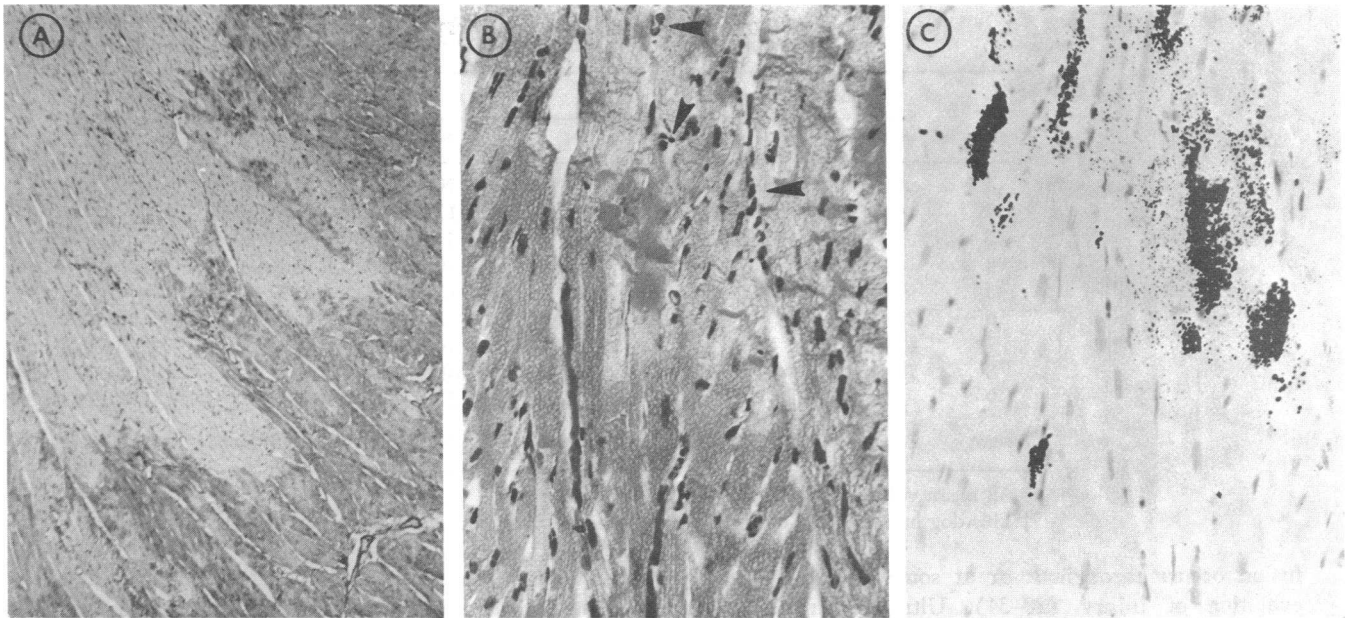


FIGURE 9 Histologic sections through the edge of an acute canine infarct, 42 h old, containing areas of necrotic and ischemic myocardium (Dog 6, Table I). In a section stained by the PAS method (A), necrotic muscle (left) appears pale due to a combination of total glycogen depletion and faint diffuse PAS staining. Adjacent ischemic muscle contains variable amounts of darkly stained glycogen deposits. The foci of necrotic myocardium show neutrophilic infiltration (arrowheads; B) and contain muscle cells with disrupted myofibrils and calcium deposits (C). Adjacent ischemic myocardium is devoid of neutrophils. Ischemic muscle cells do not contain calcium deposits but exhibit fine vacuolization suggestive of lipid accumulation. A, PAS stain,  $\times 60$ ; B, hematoxylin and eosin,  $\times 300$ ; and C, von Kossa stain,  $\times 300$ .

8% of normal in the inner peripheries, and 3% of normal in the centers of the infarcts.

Maximal concentration of  $^{99m}\text{Tc}$ -PYP in the nine transmural infarcts occurred in the outer peripheral zones which exhibited variable degrees of residual blood flow. Average mean  $^{99m}\text{Tc}$ -PYP uptake was 21.5 times normal in partially necrotic areas in the outer peripheries of the infarcts, 24.5 times normal in areas of extensive to homogeneous necrosis in the outer peripheries, 7.8 times normal in the inner peripheries, and 1.7 times normal in the centers of the infarcts.

In the 1 heart with a subendocardial infarct, subepicardial regions with patchy necrosis exhibited a mean 50% reduction in blood flow (range 0.16–1.16,  $n = 6$ ) as measured by microspheres and mean  $^{99m}\text{Tc}$ -PYP uptake of 3.8 times normal (range 1.3–9.3,  $n = 6$ ); however, subendocardial regions with extensive to homogeneous necrosis showed markedly reduced blood flow (mean 13% of normal, range 0.00–0.30,  $n = 14$ ) and marked concentration of  $^{99m}\text{Tc}$ -PYP (mean level of 21.4 times normal, range 11.2–33.9,  $n = 14$ ).

In the 10 infarcts, maximal abnormal-to-normal levels of  $^{99m}\text{Tc}$ -PYP were 19.4, 16.8, 17.4, 10.2, 26.3, 63.7, 82.2, 105.1, 37.8, and 33.9, respectively (average 41.3). In each heart, the area of maximal  $^{99m}\text{Tc}$ -PYP concentra-

tion corresponded to a region of extensive or confluent necrosis with prominent calcification.

## DISCUSSION

This study demonstrates that the status of regional myocardial perfusion after coronary occlusion is a key determinant for the occurrence of distinctive morphologic patterns of necrosis in different regions of acute myocardial infarcts and for the scintigraphic detection of such infarcts with  $^{99m}\text{Tc}$ -PYP and  $^{201}\text{Tl}$ . These observations extend previously reported work (4, 7, 24, 24a) regarding the interrelationships of regional flow alterations and uptake of various radiopharmaceuticals by relating these phenomena to the extent and nature of the associated myocardial damage.

The occurrence of significant levels of perfusion in the outer peripheral zones of the transmural infarcts is explicable on the basis of collateral blood flow to these regions (25–27). Residual blood flow in the outer peripheries correlated with the presence of numerous irreversibly injured muscle cells with contraction bands and calcium deposits. Previous experimental studies have indicated that necrosis with contraction band formation and, frequently, calcification, develops when myocardial per-

TABLE I  
Mean Abnormal-to-Normal Ratios of <sup>99m</sup>Tc-PYP, <sup>201</sup>Tl, and <sup>125</sup>I-Microspheres in

Dog	Outer periphery with 1-2+ necrosis			Outer periphery with 3-4+ necrosis		
	<sup>99m</sup> Tc-PYP	<sup>201</sup> Tl	<sup>125</sup> I	<sup>99m</sup> Tc-PYP	<sup>201</sup> Tl	<sup>125</sup> I
1	6.2±0.7*	0.76±0.04		10.4±1.2	0.19±0.03	
2	6.8±0.8	0.81±0.05		12.5±1.1	0.31±0.05	
3	7.4±1.7	0.75±0.06		11.9±1.1	0.24±0.03	
4	3.8±0.9	0.69±0.06		6.9±1.0	0.36±0.05	
5	7.8±0.9	0.71±0.04		15.3±1.7	0.27±0.03	
6	24.7±5.0		0.93±0.08	32.9±5.9		0.14±0.05
7†	42.2±6.9		0.64±0.06	49.8±8.6		0.25±0.03
8	79.6±8.0		0.64±0.06	58.5±14.3		0.34±0.05
9	14.9		1.03	23.1±3.2		0.31±0.04
Average	21.5±8.3	0.74±0.02	0.81±0.10	24.5±6.2	0.27±0.03	0.26±0.04

\* All mean values are accompanied by standard errors.

† This dog had an 18-hr-old myocardial infarct. Other dogs had approximately 42-hr-old infarcts.

fusion occurs throughout or at some time during the evolution of injury (28-34). Ultrastructural studies from our own and other laboratories have shown that calcium deposits in the irreversibly injured muscle cells are localized to the mitochondria and occur in the form of apatite-like spicules or deposits of subcrystalline, finely granular material (35-38). In contrast to the predominant pattern of muscle cell necrosis in the outer peripheral regions of the infarcts, central regions of the infarcts with severely reduced blood flow contained necrotic muscle cells without contraction bands or calcium deposits. This pattern of myocardial necrosis previously has been shown to be typical of areas rendered maximally ischemic by permanent coronary occlusion (32-34, 38-40). Such regions have also been shown to develop a severe impairment to myocardial perfusion within 90-120 min after onset of coronary occlusion (22, 28). The inner peripheral zones of the infarcts

appeared to represent transition regions between the outer peripheral and central zones, since these inner peripheral zones were characterized by considerably reduced blood flow, by necrotic muscle cells with contraction bands but usually minimal calcium deposits, and by a concentration of neutrophils along the borders with the central zones. Patterns of myocardial necrosis similar to those described in the present study also have been shown to be typical of acute myocardial infarcts in humans, although detailed analysis of calcification in human infarcts has not been reported (41-43).

Our findings with <sup>201</sup>Tl confirm the work of Strauss et al. which showed that the degree of myocardial uptake of <sup>201</sup>Tl correlates with the level of myocardial perfusion under conditions of normal or decreased coronary blood flow (7). In the present study, myocardial infarcts were readily detected as filling defects on <sup>201</sup>Tl myocardial scintigrams. Nevertheless, postmortem scintig-

TABLE II  
Statistical Analysis (Paired t Test) of Mean Values for <sup>99m</sup>Tc-PYP, <sup>201</sup>Tl, and <sup>125</sup>I-Microspheres in Different Regions of Nine Canine Transmural Acute Anterior

Myocardial infarcts	<sup>99m</sup> Tc-PYP (n = 9)	<sup>201</sup> Tl* (n = 5)	<sup>125</sup> I* (n = 4)
Comparison			
Outer periphery with 1-2+ necrosis vs. outer periphery with 3-4+ necrosis	NS†§	<0.001	<0.02
Outer periphery with 1-2+ necrosis vs. inner periphery	NS§	<0.001	<0.005
Outer periphery with 1-2+ necrosis vs. center	<0.05	<0.001	<0.005
Outer periphery with 3-4+ necrosis vs. inner periphery	<0.005	<0.001	<0.05
Outer periphery with 3-4+ necrosis vs. center	<0.005	<0.005	<0.02
Inner periphery vs. center	<0.005	<0.025	NS§

\* Group t test analysis revealed no significant differences in the values for <sup>201</sup>Tl and <sup>125</sup>I-microspheres in each of the four regions of the infarcts.

† When dog no. 8 is omitted from the comparison, the difference becomes significant with *P* < 0.001.

§ Differences were considered significant when *P* < 0.05.

*Different Regions of Nine Canine Transmural Acute Anterior Myocardial Infarcts*

Inner periphery with 4+ necrosis			Center with 4+ necrosis		
<sup>99m</sup> Tc-PYP	<sup>201</sup> Tl	<sup>125</sup> I	<sup>99m</sup> Tc-PYP	<sup>201</sup> Tl	<sup>125</sup> I
4.6±0.5	0.06±0.00		0.7±0.2	0.03±0.00	
2.6±0.4	0.09±0.00		0.3	0.03	
4.7±0.9	0.08±0.00		0.6±0.2	0.03±0.01	
3.3±0.9	0.13±0.03		0.5±0.0	0.03±0.00	
4.8±0.7	0.06±0.00		2.2±1.2	0.04±0.00	
10.8±1.9		0.08±0.03	2.7±0.5		0.03±0.02
8.9±0.8		0.06±0.01	1.4±0.5		0.03±0.00
21.1±6.9		0.04±0.00	4.5±0.2		0.03±0.00
9.1±0.8		0.05±0.02	2.1±0.8		0.05±0.00
7.8±1.9	0.08±0.01	0.06±0.01	1.7±0.5	0.03±0.00	0.04±0.01

raphy of whole hearts revealed considerable overlapping of <sup>201</sup>Tl activity with areas of intense <sup>99m</sup>Tc-PYP uptake which were limited to areas of myocardial infarction as discussed below. Visualization of <sup>201</sup>Tl activity in the infarct regions may have resulted from a combination of: (a) superimposition of normal and infarcted areas in the two-dimensional scintigraphic image, and (b) visualization of the significant levels of <sup>201</sup>Tl within the infarcts demonstrated by scintigraphy of ventricular slices (Fig. 5) and by well counting (Table I). The demonstration of significant <sup>201</sup>Tl activity in outer peripheral regions of the infarcts is of interest since myocardial uptake of <sup>201</sup>Tl and related radionuclides has been considered to be mediated by active membrane transport by muscle cells (44, 45). Although some foci of damaged, but not demonstrably necrotic, myocardium usually were present in the outer peripheries of the infarct, even in areas of nearly homogeneous necrosis (Fig. 7), the amount of <sup>201</sup>Tl uptake appeared to be in excess of the amount of non-necrotic myocardium in a given sample. Furthermore, one must question whether or not such damaged muscle cells can actively take up <sup>201</sup>Tl. It seems probable, therefore, that <sup>201</sup>Tl uptake in the peripheries of the infarcts, especially in regions of extensive to homogeneous necrosis, results primarily from transport across endothelium, followed by tissue sequestration in the absence of active membrane transport by muscle cells.

Thus, it would appear that accurate sizing of acute myocardial infarcts from <sup>201</sup>Tl myocardial scintigrams may prove difficult because of several factors including: (a) the fact that <sup>201</sup>Tl scintigrams show abnormalities as negative defects, (b) geometric factors resulting in superimposition of normal and infarcted regions, (c)

the lack of sharp demarcation in <sup>201</sup>Tl uptake between infarcted and normal myocardium, and (d) the lack of specificity of <sup>201</sup>Tl scintigraphy for the detection of areas of acute myocardial infarction alone. A corollary of the flow-related nature of myocardial scintigraphy with <sup>201</sup>Tl and related radionuclides is that filling defects on myocardial scintigrams can result from any pathologic alteration or combination of alterations associated with significantly reduced regional myocardial perfusion, including ischemia and myocardial fibrosis in addition to acute myocardial infarction (1-10).

Our findings with respect to <sup>99m</sup>Tc-PYP indicate that the scintigraphic detection of acute myocardial infarcts with this agent results from marked uptake of the radiopharmaceutical in areas with myocardial necrosis and residual perfusion. The marked concentrations of <sup>99m</sup>Tc-PYP demonstrated in the outer peripheral regions of transmural myocardial infarcts explains the doughnut patterns observed on <sup>99m</sup>Tc-PYP myocardial scintigrams in dogs with LAD occlusion, and probably, in some patients with large anterior infarcts (18, 20). Similarly, concentration of <sup>99m</sup>Tc-PYP throughout the regions of extensive necrosis in the one dog with a subendocardial infarct correlates with the homogeneous pattern of <sup>99m</sup>Tc-PYP uptake observed in patients with subendocardial infarcts (19, 20).

Although maximal concentration of <sup>99m</sup>Tc-PYP occurred in areas of extensive to homogeneous necrosis in the outer peripheral regions of canine myocardial infarcts, considerable uptake of the agent also occurred in areas composed of mixtures of necrotic and ischemic myocardium in the outer peripheries of the different infarcts. The latter finding raised the possibility that significant uptake of <sup>99m</sup>Tc-PYP occurred in damaged as well as

necrotic myocardium. Zweiman et al. also have reported that a closely related phosphorous-containing compound, technetium-99m diphosphate, shows modestly increased uptake (1–11 times normal) in ischemic myocardium with mildly reduced flow as well as intense uptake (25–52 times normal) in infarcted myocardium with more severe blood flow reduction (24). In the present study, however, some foci of myocardial necrosis were identified in all regions with increased  $^{99m}\text{Tc}$ -PYP uptake. It is also important to note that regions of partial necrosis with significant  $^{99m}\text{Tc}$ -PYP uptake involved only small areas at the edges of the infarcts and were typically located in subepicardial regions adjacent to subendocardial areas of extensive to homogeneous necrosis (Figs. 5, 6). Furthermore, the lack of correlation between extent of necrosis and  $^{99m}\text{Tc}$ -PYP uptake also could be explained by relatively greater  $^{99m}\text{Tc}$ -PYP uptake by smaller amounts of necrotic myocardium as a consequence of more abundant blood flow to these areas than to areas of homogeneous necrosis with lower levels of perfusion.

Thus, the thesis that positive  $^{99m}\text{Tc}$ -PYP myocardial scintigrams in subjects with acute myocardial infarcts result primarily from visualization of high levels of  $^{99m}\text{Tc}$ -PYP in necrotic myocardium is supported by the findings in this study as well as by: (a) the close correlation between estimates of infarct size obtained from measurements of infarct area on  $^{99m}\text{Tc}$ -PYP myocardial scintigrams and morphologically determined infarct size in dogs with proximal LAD occlusion (46, 47); (b) the findings of Martonffy et al. (48) indicating that significant  $^{99m}\text{Tc}$ -PYP concentration occurs only after intervals of ischemia which produce myocardial necrosis in the canine left circumflex coronary occlusion model (28, 38); and (c) the characteristic time course of positive  $^{99m}\text{Tc}$ -PYP myocardial scintigraphy, with positive myocardial scintigrams being observed between 12–16 h and 7–14 days after experimental LAD occlusion or clinical onset of infarction (16–20, 35).

The present study also confirms and extends our previous work indicating a temporal and topographical relationship between calcium accumulation and concentration of  $^{99m}\text{Tc}$ -PYP in acute myocardial infarcts (35). Our findings indicate that  $^{99m}\text{Tc}$ -PYP concentration is related to the presence of mitochondrial calcification in irreversibly injured muscle cells (35), but not necessarily to the total calcium content in a given region of infarcted myocardium, since  $^{99m}\text{Tc}$ -PYP concentration and mitochondrial calcification occur only in peripheral regions of large canine infarcts and not in central regions which may contain variable amounts of calcium deposits in walls of small blood vessels and tissue spaces. The present study also demonstrates that  $^{99m}\text{Tc}$ -PYP concentration in acute infarcts is more directly related

to calcium accumulation in necrotic muscle cells rather than to neutrophilic infiltration, since inner peripheral zones of the infarcts exhibited much higher ratios of neutrophils to calcified muscle cells but much lower levels of  $^{99m}\text{Tc}$ -PYP as compared to the outer peripheral zones.

Nevertheless, establishment of a definitive relationship between the extent of muscle cell calcification and the degree of  $^{99m}\text{Tc}$ -PYP uptake was complicated by variations in abnormal-to-normal ratios of  $^{99m}\text{Tc}$ -PYP and in extent of muscle cell calcification in different hearts. Furthermore, extent of calcium accumulation in the infarcts was evaluated only by the von Kossa stain, a histochemical technique which is limited to detection of relatively large calcium-containing precipitates which remain in tissues after fixation and histologic processing (23). It also should be pointed out that the present study does not clarify the possible role of myocardial calcification in the development of positive  $^{99m}\text{Tc}$ -PYP myocardial scintigrams in some patients with unstable angina pectoris (20) and in some patients with ventricular aneurysms (49). Thus, the available data indicate that uptake of  $^{99m}\text{Tc}$ -PYP into calcium depositis can play an important role in the concentration of the radionuclide in damaged myocardium, but do not exclude the possibility that another mechanism(s) also may be involved in this phenomenon. It is possible, for example, that concentration of  $^{99m}\text{Tc}$ -PYP may be mediated by influx of the agent along with calcium ions, followed by formation of an intracellular calcium pyrophosphate complex, incorporation of the radiopharmaceutical into foci of calcification, and (or) binding of the agent by altered intracellular macromolecules (50, 51).

Comparison of the present experimental findings obtained in dogs with the results of combined  $^{201}\text{Tl}$  and  $^{99m}\text{Tc}$ -PYP scintigraphy of patients with clinically documented acute myocardial infarction has revealed generally similar scintigraphic findings in the experimental animals and patients (10). Nevertheless, several patients with acute myocardial infarcts have shown filling defects on  $^{201}\text{Tl}$  myocardial scintigrams which were larger than the areas of  $^{99m}\text{Tc}$ -PYP activity, suggesting the presence of significant areas of fibrosis or ischemia as well as acute infarction in these patients (10). Thus, the findings in our experimental and clinical studies support the conclusions that: (a)  $^{99m}\text{Tc}$ -PYP myocardial scintigrams visualize acute myocardial infarcts more specifically than  $^{201}\text{Tl}$  myocardial scintigrams; (b)  $^{201}\text{Tl}$  myocardial scintigrams detect a spectrum of lesions, including old myocardial infarcts and areas of ischemia in addition to acute myocardial infarcts; and (c) the combined use of both the  $^{99m}\text{Tc}$ -PYP and  $^{201}\text{Tl}$  scintigraphic techniques provides a more complete scintigraphic evaluation of patients with ischemic heart disease.

## ACKNOWLEDGMENTS

We gratefully acknowledge the help of Ms. Anna Reynolds who was responsible for preparation of the large numbers of histologic sections needed for this study. We also thank Miss Judy Ober, Mrs. Dorothy Gutekunst, Mrs. Patti Duke, Miss Janice McNatt, Mr. Curtis Garner, and Mr. Gifford Ramsey for expert technical assistance in the performance of the animal experiments, Mrs. Linda Bolding for preparation of the photomicrographs, and Miss Kathy Handrick, Mrs. Donna Place, and Mrs. Belinda Lambert for secretarial assistance.

This work was supported, in part, by the Harry S. Moss Heart Fund, National Institutes of Health Ischemic Heart Disease Specialized Center of Research (SCOR) grant HL 17669, National Institutes of Health grant HL 17777, and the Southwestern Medical Foundation.

## REFERENCES

- Zaret, B. L. 1974. Radionuclides and regional myocardial perfusion. *Am. J. Med. Sci.* **267**: 138-149.
- Strauss, H. W., B. L. Zaret, N. D. Martin, H. P. Wells, Jr., and M. D. Flamm, Jr. 1973. Noninvasive evaluation of regional myocardial perfusion with potassium 43. Technique in patients with exercise-induced transient myocardial ischemia. *Radiology.* **108**: 85-90.
- Zaret, B. L., H. W. Strauss, N. D. Martin, H. P. Wells, Jr., and M. D. Flamm, Jr. 1973. Noninvasive regional myocardial perfusion with radioactive potassium. Study of patients at rest, with exercise and during angina pectoris. *N. Engl. J. Med.* **288**: 809-812.
- Prokop, E. K., H. W. Strauss, J. Shaw, B. Pitt, and H. N. Wagner, Jr. 1974. Comparison of regional myocardial perfusion determined by ionic potassium-43 to that determined by microspheres. *Circulation.* **50**: 978-984.
- Martin, N. D., B. L. Zaret, R. L. McGowan, H. P. Wells, Jr., and M. D. Flamm, Jr. 1974. Rubidium-81: a new myocardial scanning agent. Noninvasive regional myocardial perfusion scans at rest and exercise and comparison with potassium-43. *Radiology.* **111**: 651-656.
- Romhilt, D. W., R. J. Adolph, V. J. Sodd, N. I. Levenson, L. S. August, H. Nishiyama, and R. A. Berke. 1973. Cesium-129 myocardial scintigraphy to detect myocardial infarction. *Circulation.* **48**: 1242-1251.
- Strauss, H. W., K. Harrison, J. K. Langan, E. Lebowitz, and B. Pitt. 1975. Thallium-201 for myocardial imaging. Relation of thallium-201 to regional myocardial perfusion. *Circulation.* **51**: 641-645.
- Jambroes, G., P. P. v. Rijk, C. J. M. v.d. Berg, C. N. d. Graaf, and A. N. E. Zimmerman. 1975. Improved scintiphotography of the heart using thallium-201. *J. Nucl. Med.* **16**: 539. (Abstr.)
- Wackers, F. J.Th., J. B. v.d. Schoot, E. B. Sokole, G. Samson, G. J. C. v. Niftrik, K. I. Lie, D. Durrer, and H. J. J. Wellens. 1975. Noninvasive visualization of acute myocardial infarction in man with thallium-201. *Br. Heart J.* **37**: 741-744.
- Parkey, R. W., F. J. Bonte, E. M. Stokely, S. E. Lewis, L. M. Buja, and J. T. Willerson. 1975. Acute myocardial infarction imaged with both technetium-99m stannous pyrophosphate and thallium-201: a clinical evaluation. *Circulation.* **52**(Suppl. II): II-71. (Abstr.)
- Kramer, R. J., R. E. Goldstein, J. W. Hirshfeld, Jr., W. C. Roberts, G. S. Johnston, and S. E. Epstein. 1974. Accumulation of gallium-67 in regions of acute myocardial infarction. *Am. J. Cardiol.* **33**: 861-867.
- Holman, B. L., M. K. Dewanjee, J. Idoine, C. P. Fliegel, M. A. Davis, S. Treves, and P. Eldh. 1973. Detection and localization of experimental myocardial infarction with <sup>99m</sup>Tc-tetracycline. *J. Nucl. Med.* **14**: 595-599.
- Holman, B. L., M. Lesch, F. G. Zweiman, J. Temte, B. Lown, and R. Gorlin. 1974. Detection and sizing of acute myocardial infarcts with <sup>99m</sup>Tc(Sn) tetracycline. *N. Engl. J. Med.* **291**: 159-163.
- Fink/Bennett, D., H. J. Dworkin, and Y-H. Lee. 1974. Myocardial imaging of the acute infarct. *Radiology.* **113**: 449-450.
- Rossmann, D. J., J. Rouleau, H. W. Strauss, and B. Pitt. 1975. Detection and size estimation of acute myocardial infarction using <sup>99m</sup>Tc-glucoheptonate. *J. Nucl. Med.* **16**: 980-985.
- Bonte, F. J., R. W. Parkey, K. D. Graham, and J. G. Moore. 1975. Distributions of several agents useful in imaging myocardial infarcts. *J. Nucl. Med.* **16**: 132-135.
- Bonte, F. J., R. W. Parkey, K. D. Graham, J. Moore, and E. M. Stokely. 1974. A new method for radionuclide imaging of myocardial infarcts. *Radiology.* **110**: 473-474.
- Parkey, R. W., F. J. Bonte, S. L. Meyer, J. M. Atkins, G. L. Curry, E. M. Stokely, and J. T. Willerson. 1974. A new method for radionuclide imaging of acute myocardial infarction in humans. *Circulation.* **50**: 540-546.
- Willerson, J. T., R. W. Parkey, F. J. Bonte, S. L. Meyer, and E. M. Stokely. 1975. Acute subendocardial myocardial infarction in patients. Its detection by technetium 99-m stannous pyrophosphate myocardial scintigrams. *Circulation.* **51**: 436-441.
- Willerson, J. T., R. W. Parkey, F. J. Bonte, S. L. Meyer, J. M. Atkins, and E. M. Stokely. 1975. Technetium stannous pyrophosphate myocardial scintigrams in patients with chest pain of varying etiology. *Circulation.* **51**: 1046-1052.
- Fortuin, N. J., S. Kaihara, L. C. Becker, and B. Pitt. 1971. Regional myocardial blood flow in the dog studied with radioactive microspheres. *Cardiovasc. Res.* **5**: 331-336.
- Willerson, J. T., J. T. Watson, I. Hutton, G. H. Templeton, and D. E. Fixler. 1975. Reduced myocardial reflow and increased coronary vascular resistance following prolonged myocardial ischemia in the dog. *Circ. Res.* **36**: 771-781.
- Lillie, R. D. 1965. *Histopathologic Technique and Practical Histochemistry.* McGraw-Hill, Inc., New York. 3rd edition. 198-202, 436-440.
- Zweiman, F. G., B. L. Holman, A. O'Keefe, and J. Idoine. 1975. Selective uptake of <sup>99m</sup>Tc complexes and <sup>67</sup>Ga in acutely infarcted myocardium. *J. Nucl. Med.* **16**: 975-979.
- Zaret, B. L., V. C. Di Cola, R. K. Donabedian, S. Puri, S. Wolfson, G. S. Freedman, and L. S. Cohen. 1976. Dual radionuclide study of myocardial infarction: relationships between myocardial uptake of potassium-43, technetium-99m stannous pyrophosphate, regional myocardial blood flow and creatine phosphokinase depletion. *Circulation.* **53**: 422-427.
- Bloor, C. M. 1974. Functional significance of the coronary collateral circulation. A review. *Am. J. Pathol.* **76**: 562-588.
- Gregg, D. E. 1974. The natural history of coronary collateral development. *Circ. Res.* **35**: 335-344.
- Cox, J. L., H. I. Pass, A. S. Wechsler, H. N. Oldham, Jr., and D. C. Sabiston, Jr. 1975. Coronary collateral blood

- flow in acute myocardial infarction. *J. Thorac. Cardiovasc. Surg.* 69: 117-125.
28. Kloner, R. A., C. E. Ganote, and R. B. Jennings. 1974. The "no-reflow" phenomenon after temporary coronary occlusion in the dog. *J. Clin. Invest.* 54: 1496-1508.
  29. Reichenbach, D. D., and E. P. Benditt. 1970. Catecholamines and cardiomyopathy: the pathogenesis and potential importance of myofibrillar degeneration. *Hum. Pathol.* 1: 125-150.
  30. Buja, L. M., S. Levitsky, V. J. Ferrans, S. G. Souther, W. C. Roberts, and A. G. Morrow. 1971. Acute and chronic effects of normothermic anoxia on canine hearts. Light and electron microscopic evaluation. *Circulation.* 43 and 44 (Suppl. 1): I-44-1-50.
  31. Buja, L. M., V. J. Ferrans, and R. G. Graw, Jr. 1976. Cardiac pathologic findings in patients treated with bone marrow transplantation. *Hum. Pathol.* 7: 17-45.
  32. Korb, G., and V. Totović. 1969. Electron microscopical studies on experimental ischemic lesions of the heart. *Ann. N. Y. Acad. Sci.* 156: 48-60.
  33. Heggveit, H. A. 1969. Contributions of electron microscopy to the study of myocardial ischemia. *Bull. W. H. O.* 41: 865-872.
  34. Ferrans, V. J., and W. C. Roberts. 1971/72. Myocardial ultrastructure in acute and chronic hypoxia. *Cardiology.* 56: 144-160.
  35. Buja, L. M., R. W. Parkey, J. H. Dees, E. M. Stokely, R. A. Harris, Jr., F. J. Bonte, and J. T. Willerson. 1975. Morphologic correlates of technetium-99m stannous pyrophosphate imaging of acute myocardial infarcts in dogs. *Circulation.* 52: 596-607.
  36. Buja, L. M., J. H. Dees, D. F. Harling, and J. T. Willerson. 1976. Analytical electron microscopic study of mitochondrial inclusions in canine myocardial infarcts. *J. Histochem. Cytochem.* 24: 508-516.
  37. D'Agostino, A. N., and M. Chiga. 1970. Mitochondrial mineralization in human myocardium. *Am. J. Clin. Pathol.* 53: 820-824.
  38. Shen, A. C., and R. B. Jennings. 1972. Myocardial calcium and magnesium in acute ischemic injury. *Am. J. Pathol.* 67: 417-440.
  39. Bryant, R. E., W. A. Thomas, and R. M. O'Neal. 1958. An electron microscopic study of myocardial ischemia in the rat. *Circ. Res.* 6: 699-709.
  40. Caulfield, J., and B. Klionsky. 1959. Myocardial ischemia and early infarction: an electron microscopic study. *Am. J. Pathol.* 35: 489-523.
  41. Mallory, G. K., P. D. White, and J. Salcedo-Salgar. 1939. The speed of healing of myocardial infarction. A study of the pathologic anatomy in seventy-two cases. *Am. Heart J.* 18: 647-671.
  42. Lodge-Patch, I. 1951. The ageing of cardiac infarcts, and its influence on cardiac rupture. *Br. Heart J.* 13: 37-42.
  43. Baroldi, G. 1975. Different types of myocardial necrosis in coronary heart disease: a pathophysiologic review of their functional significance. *Am. Heart J.* 89: 742-752.
  44. Schelbert, H. R., W. L. Ashburn, D. M. Chauncey, and S. E. Halpern. 1974. Comparative myocardial uptake of intravenously administered radionuclides. *J. Nucl. Med.* 15: 1092-1100.
  45. Levenson, N. I., R. J. Adolph, D. W. Romhilt, M. Gabel, V. J. Sodd, and L. S. August. 1975. Effects of myocardial hypoxia and ischemia on myocardial scintigraphy. *Am. J. Cardiol.* 35: 251-257.
  46. Stokely, E. M., L. M. Buja, S. E. Lewis, R. W. Parkey, F. J. Bonte, R. A. Harris, Jr., and J. T. Willerson. 1976. Measurement of acute myocardial infarcts in dogs with <sup>99m</sup>Tc-stannous pyrophosphate myocardial scintigrams. *J. Nucl. Med.* 17: 1-5.
  47. Botvinick, E. H., D. Shames, H. Lappin, J. V. Tyberg, R. Townsend, and W. W. Parmley. 1975. Noninvasive quantitation of myocardial infarction with technetium 99m pyrophosphate. *Circulation.* 52: 909-915.
  48. Martonffy, K., K. A. Reimer, R. E. Henkin, R. B. Jennings, and J. L. Quinn. 1975. Technetium-99m pyrophosphate concentration in experimental myocardial infarcts. *J. Nucl. Med.* 16: 548. (Abstr.)
  49. Ahmad, M., J. Dubiel, T. A. Verdon, and R. H. Martin. 1975. Technetium-99m stannous pyrophosphate myocardial imaging in patients with left ventricular aneurysm. *Clin. Res.* 23: 168A. (Abstr.)
  50. Dewanjee, M. K., and E. W. Prince. 1974. Cellular necrosis model in tissue culture: uptake of <sup>99m</sup>Tc-tetracycline and the pertechnetate ion. *J. Nucl. Med.* 15: 577-581.
  51. Dewanjee, M. K., P. C. Kahn, U. Dewanjee, and R. J. Connolly. 1975. Mechanism of localization of Tc-99m labeled pyrophosphate and tetracycline in infarcted myocardium. *J. Nucl. Med.* 16: 525. (Abstr.)